

3d and r, z Particle Simulation of Beams for Heavy Ion Fusion: the WARP Code*

A. Friedman, D. P. Grote, D. A. Callahan, and A. B. Langdon
Lawrence Livermore National Laboratory
I. Haber
U.S. Naval Research Laboratory

Abstract

WARP is an electrostatic particle-in-cell (PIC) code that is optimized for studies of space-charge-dominated beams. We use the code to understand a number of issues in HIF accelerators and transport systems, including: drift-compression in the presence of misalignments, axial confinement, longitudinal stability, transport around bends, and thermal equilibration processes. In this paper we describe the code architecture and numerical techniques employed to enhance efficiency. We then describe our new simple algorithm for following a beam around a bend, and recent results on bent-beam dynamics and transverse emittance evolution. Finally, we describe the code's most recent feature, a general-lattice capability structured to preserve the efficiency of the particle advance, and present initial results using it.

I. Introduction

In Heavy Ion inertial confinement Fusion (HIF) drivers, space-charge-dominated beams are to be accelerated and transported over large distances. WARP[1, 2, 3, 4, 5] was developed specifically for the study of emittance growth resulting from the nonlinear self-fields of such beams.

This work has recently been described in the Proceedings of the International Symposium on Heavy Ion Inertial Fusion.[3, 4, 5] In this Conference Record we briefly review the code concept, methods, and applications. We then describe new capabilities: the inclusion of a bent beam and pipe into the particle dynamics and self-field, and a general accelerator lattice. Early results using these features are described; these suggest that it may be possible to transport an axially-cool space-charge-dominated beam around a sharp bend without unacceptable emittance growth.

II. Code Overview

The WARP code contains a number of distinct parts, including: a 3d PIC package, WARP6, which uses a "warped Cartesian" mesh in x, y, z to describe bends; an axisymmetric r, z PIC package, WARPRZ; an envelope equation solver (used for loading a "matched" beam); and facilities for initialization, diagnostics, etc. In this paper we focus almost exclusively on WARP6.

*This work was performed under the auspices of the U.S. D.O.E. by Lawrence Livermore National Laboratory under contract W-7405-ENG-48, and by the Naval Research Laboratory under Lawrence Berkeley Laboratory contract DE-AC03-76SF0098.

The simulation takes place in the laboratory frame. The computational mesh fills a moving window and is laid down anew at each timestep. The self-field is assumed electrostatic; boundary conditions are those of a square metal pipe. A round pipe (via capacity matrix) is an option.

In 3d, efficiency is a critical requirement; to this end we employ a number of means, summarized here:

In leapfrog motion, if a particle were to land within a sharp-edged focusing or bending element on four steps while its neighbor did so on only three, they would receive dramatically different impulses. Thus, the advance incorporates "residence corrections" for element forces which account for the fraction of the velocity advance step actually spent within the element. This allows much bigger steps than otherwise would be possible.

No mesh arrays for the electric field components are used; instead, the electrostatic potential ϕ is differenced on a particle-by-particle basis, obviating three 3d arrays.

The FFT fieldsolver is fully vectorized and uses no scratch space. The particle advance is vectorized. Deposition of the charge density ρ is vectorized with length 8, over cells overlapped by each particle.

III. Summary of Applications

In addition to the bent-beam modeling described below, current studies include the following areas:

Drift Compression: (current enhancement resulting from a head-to-tail velocity gradient or "tilt"): Relatively small misalignments of the focusing quadrupoles can lead to significant off-axis displacements. Image forces and fringing fields can then induce emittance growth. We seek to learn how fast and how much the beam may be compressed without unacceptable emittance degradation.[1, 2]

Equilibration: We are examining the transfer of thermal energy between transverse and longitudinal motions. For certain ranges of physical parameters, a beam initialized colder in z (axially) than in x, y (transversely) is observed to heat rapidly in z until T_z is a large fraction of $T_{x,y}$. This appears to be a collective process.[2, 3]

Axial Confinement, Nature of Equilibria: To follow a finite-length beam for a long time, it is necessary to apply an axial confining force. We have had success in modeling near-equilibrium beams that remain "quiescent" over runs as long as 175 lattice periods without significant emittance degradation in the simulation.[4]

Simulations of the MBE-4 Experiment: In this LBL experiment, emittance growth has been observed to accompany aggressive drift compression. Using WARP, we have been investigating mechanisms (such as axial mixing and dodecapole fields) which may be contributory.

Longitudinal Stability with Finite Gap Impedance: A new, fully causal model has been incorporated into WARPRZ, and we are beginning to study the effects of finite geometry on weakly unstable modes.[5]

IV. Bent Beam and General Lattice

We have developed a family of techniques for modeling bends. These are based upon following a particle's position and velocity in a sequence of rotated inertial (laboratory) frames. An "exact" method, which is symplectic and independent of aspect ratio, has been described previously, for both 3d and 2d (transverse) applications.[6] Here, we summarize the inexact, "simplified" method now in use.[3] We have also developed an efficient method for following a large number of particles through a general accelerator lattice in a PIC code, and briefly outline our approach.

1. Bent-beam dynamics

The radius of curvature of the reference orbit (usually the vessel centerline) is $r_* \equiv h^{-1}$. Time is the independent variable for particle orbits. The conventional (for accelerator codes) independent variable s is in WARP a dependent variable for orbits, as are x, y . In straight sections, $s \equiv z$, while in bends, $s \equiv -r_*\theta$. The "radial" coordinate is $x \equiv r - r_*$; the unit vectors \hat{x} and \hat{s} evolve as a particle moves, and are different for each particle. The axial speed is $v_z = -r\dot{\theta}$ (we use subscripts z and s interchangeably). The axial position is advanced in time using:

$$ds/dt = -r_*\dot{\theta} = (r_*/r)v_z . \quad (1)$$

In our coordinate system:

$$\frac{d}{dt}v_x = \frac{v_z^2}{r_* + x} + \frac{q}{m}\{\mathbf{E} + \mathbf{v} \times \mathbf{B}\}_x . \quad (2)$$

$$\frac{d}{dt}v_z = -\frac{v_z v_x}{r_* + x} + \frac{q}{m}\{\mathbf{E} + \mathbf{v} \times \mathbf{B}\}_z . \quad (3)$$

Note there is no factor of two in the Coriolis force; particle velocities retain their laboratory-frame magnitudes.[3] Considering only the "pseudo-force" terms, one obtains a pure rotation with the rate of change of the velocity angle:

$$\frac{d}{dt} \arctan\left(\frac{v_x}{v_z}\right) = \frac{v_z}{r_* + x} . \quad (4)$$

We thus need only augment the dipole (bending) field at each particle position with a "pseudo-gyrofrequency":

$$B_y \Leftarrow B_y - \frac{m}{q} \frac{v_z}{r_* + x} . \quad (5)$$

This folds the necessary back-rotation into existing coding. The algorithm is inexact because v_z and x change during the step, but is accurate enough for our needs; "residence corrections" on entry to and exit from bends are necessary.

2. Bent-beam self-field

Poisson's equation in "warped" coordinates is [7]:

$$\frac{1}{1 + hx} \frac{\partial}{\partial x} \left((1 + hx) \frac{\partial \phi}{\partial x} \right) + \frac{\partial^2 \phi}{\partial y^2} + \frac{1}{1 + hx} \frac{\partial}{\partial s} \left(\frac{1}{1 + hx} \frac{\partial \phi}{\partial s} \right) = -4\pi\rho . \quad (6)$$

Expanding the derivatives, we solve this iteratively. At each iteration the 3d FFT Poisson solver inverts the dominant "Cartesian" second derivative terms. The latest available iterate for ϕ (starting with ϕ of the previous timestep) is used to explicitly compute the smaller "non-Cartesian" terms, which are brought into the right member and augmented ρ . One term, proportional to $(\partial h/\partial s)(\partial \phi/\partial s)$, is included by a simple finite difference, assuming the change in h at bend entry/exit can be spread in s slightly. The iteration converges rapidly, typically reaching relative changes in ϕ of 10^{-6} in two or three passes; this corresponds to a typical relative error in the Poisson equation of $\sim 10^{-8}$, which is more than adequate.

It is necessary to obtain the true charge density from the "conventional" ρ_c collected from the particles, using $\rho = \rho_c r_*/r$, since (in a bend) the separation in s of zones varies with x . Also, the axial field is $E_z = -(r_*/r)\partial \phi/\partial s$.

3. General accelerator lattice for PIC

Until recently WARP allowed only a limited, highly regular lattice; a general lattice of arbitrarily-located sharp-edged elements has now supplanted it. At each particle location, the field from each type of lattice element (quadrupole, dipole, bend, etc.) is obtained algebraically and added to the total; residence corrections are included. Dipoles (fields) are independent of bends (curves in the reference orbit), but may optionally be inferred from them. Focusing in y by angled dipole faces is implemented via thin-lens corrections. Elements of different types may overlap each other.

Since each particle is at different s , efficiency precludes searching for element data on a particle-by-particle basis. At the beginning of each timestep, a number of co-moving 1d arrays, one for each property of each element type, are set. These arrays are comprised of cells having uniform size Δs ; a cell contains data describing the nearest element of the corresponding type. Then, for each particle the code computes a cell index j using a greatest-integer function applied to its $s/\Delta s$. The properties of relevant elements are then directly available. For example, the position of the left edge ("start") of the nearest quadrupole element is retrieved from cell j of array $cquadzs$. The rapid "gather" capability of (e.g.) the Cray X/MP is thus usable.

V. Examples

A first example illustrates the effect of bent-beam self-fields on a space-charge-dominated beam moving around a bend. The bend is 3.6 m (3 FODO periods) long, and has radius $r_* = 3.6/\pi = 1.146$ m. The uniform bending field

of 1.375 T fills a half-space; it acts on the beam between $s = 1.2$ m and $s = 4.8$ m (i.e., the dipole B_y is superposed over the 20 cm magnets and 40 cm drifts of the FODO lattice). The undepressed tune (phase advance per lattice period) is $\sigma_0 = 60^\circ$, the depressed tune $\sigma = 20^\circ$; the ratio of space charge to emittance forces is about 6:1. The runs use a $64 \times 64 \times 128$ mesh, with square walls at ± 9 cm; 54160 simulation particles; and a timestep size Δt corresponding to 2 cm/step. The runs follow an axially cold "cigar" beam with a K-V transverse distribution[4], assuming singly-charged carbon, 5.2 A, 10^7 eV (speed 1.27×10^7 m/s). The beam starts out 1.5 m long; its ends expand due to electrostatic repulsion, but the rarefaction does not reach pulse center by the end of the run, after 300 steps (6 m).

Figure 1 depicts the evolution of the mid-pulse x - x' emittance for a straight beam (lowest curve); a bent beam in a straight-beam self-field, retaining only the Cartesian terms in Poisson's equation (middle curve); and a bent beam in a consistent self-field (upper curve). The pulse center enters the bend $1/5^{\text{th}}$ of the way through the run, at $t = 0.095 \mu\text{s}$; shortly thereafter, the emittance jumps slightly. In the middle of the bend (and the run), sector-magnet focusing renders this (un-matched) beam very thin in x . The pulse center leaves the bend at $t = 0.379 \mu\text{s}$. Some of the structure in these curves is due to statistical noise. Nonetheless, it is clear that the emittance growth is small, but greatest for a bent-beam in a consistent field.

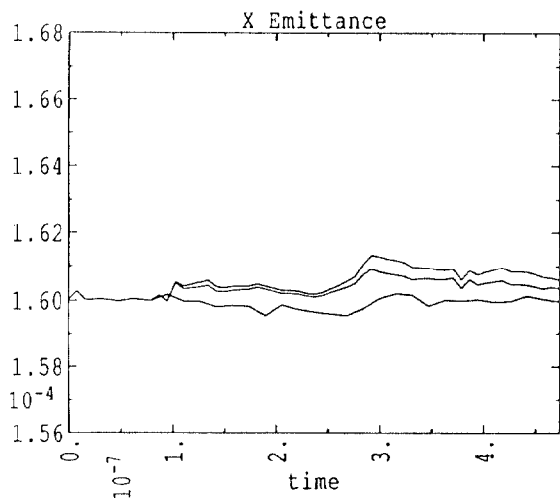


Figure 1: Straight beam vs. bent beam in straight field vs. bent beam in bent field, simple bend.

In a second example, we examine beam behavior in a lattice similar to one studied earlier for the upcoming ILSE experiments.[8] Our lattice differs from that of the reference; most notably, it uses sector magnets instead of "box" dipoles and is an imperfect achromat. For this system, $\sigma_0 = 72^\circ$, $\sigma = 20^\circ$, and dipoles (20 cm) and quadrupoles (20 cm) alternate in a FOBOBO lattice with full period 1.2 m. The first dipole begins at $z = 2.6$ m, the last ends at 16.6 m (after 180° of bending), and we end the run at 18 m (900 steps). Here, we consider axially-cold and -hot ($T_z \sim T_\perp$) beams. Results are shown in Figure 2; there is clearly emittance growth for the axially-hot beam (upper

curve); although it appears to die out, in fact it is observed to couple into the y direction, and ϵ_y (not shown) grows to $9.15 \times 10^{-5} \pi\text{m-rad}$ as ϵ_x decays. An axially-hot straight beam in a similar lattice without dipoles is not observed to suffer emittance growth.

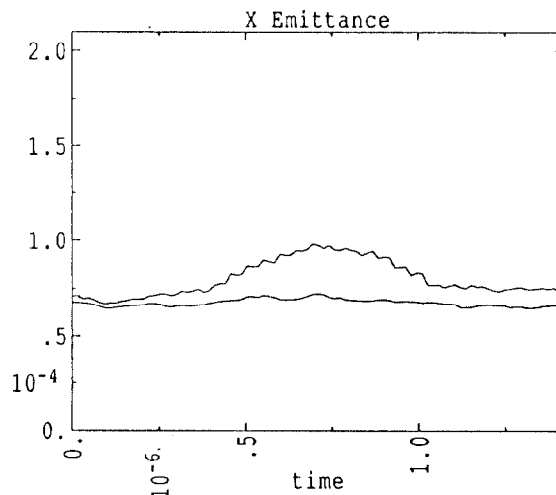


Figure 2: Axially-hot vs. -cold beam, ILSE-like lattice.

Note that these figures differ from those presented previously in that they employ a new, superior emittance diagnostic. This maps particle $\{\mathbf{x}, \mathbf{v}\}$'s to a common s before taking moments. It allows particles from a wider range in s to be included with less spurious rotation of the phase ellipse, giving better statistics and much smoother plots.

These results suggest that a carefully matched achromat design which takes self-field effects into account may be important. Nonetheless, we continue to be encouraged by the small emittance growth in the axially-cold runs, which use sharp bends, crude lattices, and unmatched beams.

References

- [1] A. Friedman, D. A. Callahan, D. P. Grote, A. B. Langdon, and I. Haber, *Proc. Conf. on Computer Codes and the Linear Accelerator Community*, Los Alamos NM, January 21–25, 1990.
- [2] A. Friedman, R. O. Bangerter, D. A. Callahan, D. P. Grote, A. B. Langdon, and I. Haber, *Proc. 2nd European Particle Accelerator Conference*, Nice, June 12–16, 1990.
- [3] A. Friedman, D. A. Callahan, D. P. Grote, A. B. Langdon, and I. Haber, *Proc. International Symposium on Heavy Ion Inertial Fusion*, Monterey, Dec. 3–6, 1990 (to be published in *Particle Accelerators*).
- [4] D. P. Grote, A. Friedman, and I. Haber, *ibid.*
- [5] D. A. Callahan, A. B. Langdon, A. Friedman, D. P. Grote, and I. Haber, *ibid.*
- [6] A. Friedman, *Proc. 13th Conf. on Numerical Simulation of Plasmas*, Santa Fe NM, 1989.
- [7] K. L. Brown and R. V. Servranckx, in *Physics of High Energy Particle Accelerators*, AIP Conf. Proc. 127, 75 (1983).
- [8] E. P. Lee, *Nucl. Inst. Meth. in Plasma Research* A278, 178 (1989).